An accurate numerical prediction of fluid flow through porous media

Nor Azwadi C. Sidik, and Mohd Irwan M. Azmi
azwadifkm@gmail.com, mohdirwan@utem.edu.my

***Abstract*—**The effects of material's porosity on the fluid flow behavior were studied numerically in detail. The method of alternative finite different scheme was employed to calculate the velocity and flow profile with high order of accuracy. The numerically calculated velocity profiles for the pure shear-driven cavity flow were compared with the benchmark solutions for the purpose of method validation. To explore the effect of material's porosity, prediction of fluid flow were made at various values of porosity and a Reynolds number in a shear-driven cavity. The numerical results of velocity profiles and plots of streamline agree well with other reported results indicated the multidisciplinary applications of the present scheme.

***Keywords*—**Navier-Stokes, porosity, cubic polynomial, numerical method, shear-driven cavity.

I. Introduction

FLUID flow through porous media for many different kinds of porosities are of great importance because of their existence in industrial applications. These existences have motivated extensive research on the fluid flow characteristics due to the presence of material's porosity.

On the other hand, the 2D fluid flow inside a square cavity filled with porous medium, which is related to a number of natural phenomena and industrial applications [1][2], is also an interesting subject. A lot of numerical simulations have been conducted to investigate the effect of porosity on fluid flow behavior. Cheng [3] provides an extensive review of literature on flow structure in fluid saturated porous media with regard to applications in geothermal systems. Nield and Bejan [4] gives an excellent summary of the subject. Other works are [5-6] and [7]. Due to the complexity of porous structure and fluid interaction with the boundaries, most of the mentioned researchers preferred numerical approach to understand the fluid flow behavior in the system. Interestingly, many of them applied conventional numerical schemes based on discretizations of the semiempirical models as their numerical tools.

A review of the available literature shows that the effects of the medium porosity on the flow structures have not been well discussed by the previous researchers. To gain better understanding on the problem in hand, the fundamental flow solution must be known. Therefore, it is the purpose of this present study to investigate the vortex dynamics of the two-dimensional flow manifold of such fluid flow problem.

II. Materials and Methods

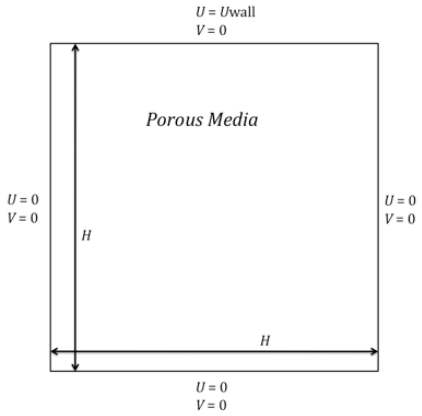

Fig. 1 Schematic geometry for shear driven fluid flow through porous media.

The physical domain of the problem is represented in Fig. 1. The top lid was constantly moved to the right direction at different constant velocity U_{wall} to give the Reynolds $(Re = U_{wall}H/\upsilon)$ number of 400. The aspect ratio was set at unity. In the present analysis, the computations are conducted on a two-dimensional plane as shown in Fig. 1. This two dimensional approximation was undertaken based on a physical assumption that the behaviour of the shear driven vortex is relatively unaffected by the three dimensionality of the flow.

In present study, the governing equation of the Brinkmann-extended Darcy formulation is considered [8]. Therefore, the governing continuity and x-and y-momentum equations can be expressed as follow

$$\frac{\partial u}{\partial x} + \frac{\partial v}{\partial y} = 0 \tag{1}$$

$$\varepsilon\frac{\partial u}{\partial t}+u\frac{\partial u}{\partial x}+v\frac{\partial u}{\partial y}=-\frac{\varepsilon^2}{\rho}\frac{\partial p}{\partial x}+\varepsilon\upsilon_f\left(\frac{\partial^2 u}{\partial x^2}+\frac{\partial^2 u}{\partial y^2}\right)-\frac{\varepsilon^2\upsilon_f}{K}u-\frac{\varepsilon^2 F}{\sqrt{K}}|\mathbf{v}|u \quad (2)$$

$$\varepsilon\frac{\partial v}{\partial t}+u\frac{\partial v}{\partial x}+v\frac{\partial v}{\partial y}=-\frac{\varepsilon^2}{\rho}\frac{\partial p}{\partial y}+\varepsilon\upsilon_f\left(\frac{\partial^2 v}{\partial x^2}+\frac{\partial^2 v}{\partial y^2}\right)-\frac{\varepsilon^2\upsilon_f}{K}v-\frac{\varepsilon^2 F}{\sqrt{K}}|\mathbf{v}|v \quad (3)$$

In this work, the pressure term in the eqns. (2) and (3) are eliminated and rewrite in terms of vorticity function as follow

$$\varepsilon\frac{\partial \omega}{\partial t}+u\frac{\partial \omega}{\partial x}+v\frac{\partial \omega}{\partial y}=\varepsilon\upsilon_f\left(\frac{\partial^2 \omega}{\partial x^2}+\frac{\partial^2 \omega}{\partial y^2}\right)-\frac{\varepsilon^2\upsilon_f}{K}\omega-\frac{\varepsilon^2 F}{\sqrt{K}}|\mathbf{v}|\omega+\frac{\varepsilon^2 F}{\sqrt{K}}\left(u\frac{\partial}{\partial y}|\mathbf{v}|-v\frac{\partial}{\partial x}|\mathbf{v}|\right) \quad (4)$$

In terms of stream function, the equation defining the vorticity becomes

$$\omega=-\left(\frac{\partial^2 \psi}{\partial x^2}+\frac{\partial^2 \psi}{\partial y^2}\right) \quad (5)$$

Before considering any numerical solution to the above set of equations, it is convenient to rewrite the equations in terms of dimensionless variables. The following dimensionless variables will be used here

$$\Psi=\frac{\psi}{u_\infty H},\ \Omega=\frac{\omega H^2 Pr}{\upsilon}$$
$$U=\frac{u}{u_\infty},\ V=\frac{v}{u_\infty} \quad (6)$$
$$X=\frac{x}{H},\ Y=\frac{y}{H},\ \tau=\frac{tu_\infty}{H}$$

In terms of these variables, Eqns. (4) and (5) become

$$\frac{\partial\Omega}{\partial\tau}+\frac{U}{\varepsilon}\frac{\partial\Omega}{\partial X}+\frac{V}{\varepsilon}\frac{\partial\Omega}{\partial Y}=\frac{1}{Re}\left(\frac{\partial^2\Omega}{\partial X^2}+\frac{\partial^2\Omega}{\partial Y^2}\right)-\frac{\varepsilon}{Da\,Re}\Omega-\frac{\varepsilon F}{\sqrt{Da}}|\mathbf{V}|\Omega+\frac{\varepsilon F}{\sqrt{Da}}\left(U\frac{\partial|\mathbf{V}|}{\partial Y}-V\frac{\partial|\mathbf{V}|}{\partial X}\right) \quad (7)$$

$$\Omega=-\left(\frac{\partial^2\Psi}{\partial X^2}+\frac{\partial^2\Psi}{\partial Y^2}\right) \quad (8)$$

where the dimensionless parameters of Darcy number, *Da* and Reynolds number, *Re* are defined as

$$Da=\frac{K}{H^2} \quad (9)$$

$$Re=\frac{u_\infty H}{\upsilon_f} \quad (10)$$

and $F=1.75/\sqrt{150\varepsilon^2}$ is the geometric function.

In this section, we begin by recalling Eqn. (7) and it's spatial derivatives, and split them into advection and nonadvection phases as follow

Advection phase:

$$\frac{\partial\Omega}{\partial\tau}=-\left(\frac{U}{\varepsilon}\frac{\partial\Omega}{\partial X}+\frac{V}{\varepsilon}\frac{\partial\Omega}{\partial Y}\right) \quad (11)$$

$$\frac{\partial\Omega_x}{\partial\tau}=-\left(\frac{U}{\varepsilon}\frac{\partial\Omega_x}{\partial X}+\frac{V}{\varepsilon}\frac{\partial\Omega_x}{\partial Y}\right) \quad (12)$$

$$\frac{\partial\Omega_y}{\partial\tau}=-\left(\frac{U}{\varepsilon}\frac{\partial\Omega_y}{\partial X}+\frac{V}{\varepsilon}\frac{\partial\Omega_y}{\partial Y}\right) \quad (13)$$

Nonadvection phase:

$$\frac{\partial\Omega}{\partial\tau}=\frac{1}{Re}\left(\frac{\partial^2\Omega}{\partial X^2}+\frac{\partial^2\Omega}{\partial Y^2}\right)-\frac{\varepsilon}{Da\,Re}\Omega-\frac{\varepsilon F}{\sqrt{Da}}|\mathbf{V}|\Omega+\frac{\varepsilon F}{\sqrt{Da}}\left(U\frac{\partial|\mathbf{V}|}{\partial Y}-V\frac{\partial|\mathbf{V}|}{\partial X}\right) \quad (14)$$

$$\frac{\partial_x\Omega}{\partial\tau}=\frac{1}{Re}\left(\frac{\partial^3\Omega}{\partial X^3}+\frac{\partial^3\Omega}{\partial X\partial Y^2}\right)-\frac{\varepsilon}{Da\,Re}\frac{\partial\Omega}{\partial X}-\frac{\varepsilon F}{\sqrt{Da}}\left(\Omega\frac{\partial|\mathbf{V}|}{\partial X}+|\mathbf{V}|\frac{\partial\Omega}{\partial X}\right)+\frac{\varepsilon F}{\sqrt{Da}}\left(\frac{\partial U}{\partial X}\frac{\partial|\mathbf{V}|}{\partial Y}+U\frac{\partial^2|\mathbf{V}|}{\partial X\partial Y}-\frac{\partial V}{\partial X}\frac{\partial|\mathbf{V}|}{\partial X}-V\frac{\partial^2|\mathbf{V}|}{\partial X^2}\right)-\frac{1}{\varepsilon}\frac{\partial U}{\partial X}\frac{\partial\Omega}{\partial X}-\frac{1}{\varepsilon}\frac{\partial V}{\partial X}\frac{\partial\Omega}{\partial Y} \quad (15)$$

$$\frac{\partial_y \Omega}{\partial \tau} = \frac{1}{Re}\left(\frac{\partial^3 \Omega}{\partial X^2 \partial Y} + \frac{\partial^3 \Omega}{\partial Y^3}\right) - \frac{\varepsilon}{Da\,Re}\frac{\partial \Omega}{\partial Y} - \frac{\varepsilon F}{\sqrt{Da}}\left(\Omega \frac{\partial |\mathbf{V}|}{\partial Y} + |\mathbf{V}|\frac{\partial \Omega}{\partial Y}\right) + \frac{\varepsilon F}{\sqrt{Da}}\left(\frac{\partial U}{\partial Y}\frac{\partial |\mathbf{V}|}{\partial Y} + U\frac{\partial^2 |\mathbf{V}|}{\partial Y^2} - \frac{\partial V}{\partial Y}\frac{\partial |\mathbf{V}|}{\partial X} - V\frac{\partial^2 |\mathbf{V}|}{\partial X \partial Y}\right) - \frac{1}{\varepsilon}\frac{\partial U}{\partial Y}\frac{\partial \Omega}{\partial X} - \frac{1}{\varepsilon}\frac{\partial V}{\partial Y}\frac{\partial \Omega}{\partial Y} \tag{16}$$

where $\Omega_x = \partial\Omega/\partial x$ and $\Omega_y = \partial\Omega/\partial y$.

In the proposed method, the advection phase of the spatial quantities in the grid interval are approximated with constrained polynomial using the value the it's spatial derivative at neighboring grid points as follow

$$F_{i,j}(X,Y) = \left[\left(a_1\tilde{X} + a_2\tilde{Y} + a_3\right)\tilde{X} + a_4\tilde{Y} + \Omega_x\right]\tilde{X} + \left[\left(a_5\tilde{Y} + a_6\tilde{X} + a_7\right)\tilde{Y} + \Omega_y\right]\tilde{Y} + \Omega \tag{17}$$

where $\tilde{X} = X - X_{i,j}$ and $\tilde{Y} = Y - Y_{i,j}$. The coefficients of a_1, $a_2, \ldots a_7$ are determined so that the interpolation function and its first derivatives are continuous at both ends. With this restriction, the numerical diffusion can be greatly reduced when the interpolated profile is constructed. The spatial derivatives are then calculated as

$$F_{x,i,j}(X,Y) = \left(3a_1\tilde{X} + 2a_2\tilde{Y} + a_3\right)\tilde{X} + \left(a_4 + a_6\tilde{Y}\right)\tilde{Y} + \Omega_x \tag{18}$$

$$F_{y,i,j}(X,Y) = \left(2a_2\tilde{Y} + a_3\right)\tilde{X} + \left(3a_5\tilde{Y} + 2a_6\tilde{X} + 2a_7\right)\tilde{Y} + \Omega_y \tag{19}$$

In two-dimensional case, the advected profile is approximated as follow

$$\Omega^n_{i,j} = F_{i,j}(X + \eta, Y + \xi) \tag{20}$$

$$\Omega^n_{x,i,j} = F_{x,i,j}(X + \eta, Y + \xi) \tag{21}$$

$$\Omega^n_{y,i,j} = F_{y,i,j}(X + \eta, Y + \xi) \tag{22}$$

where $\eta = -U\Delta\tau$ and $\xi = -V\Delta\tau$. The newly calculated spatial quantities are then be used to solve non-advection phase of Eqns. (14) to (16) and vorticity formulation of Eqn. (8). In present study, the explicit central finite different discretisation method is applied with second order accuracy in time and space. For example, the treatment for eqn. (8) is

$$\Psi^n_{i,j} = \frac{\dfrac{\Psi^n_{i+1,j} + \Psi^n_{i-1,j}}{(\Delta X)^2} + \dfrac{\Psi^n_{i,j+1} + \Psi^n_{i,j-1} + \Omega^n_{i,j}}{(\Delta X)^2}}{\dfrac{2}{(\Delta X)^2} + \dfrac{2}{(\Delta Y)^2}} \tag{23}$$

(24)

In summary, the evolution of the proposed scheme consists of three steps. The initial value of $\Omega^n_{i,j}$, $\Omega^n_{x,i,j}$ and $\Omega^n_{y,i,j}$ are specified at each grid point. Then the system evolves in the following steps;

1. Since the pre-advected value of $\Omega^n_{i,j}$, $\Omega^n_{x,i,j}$ and $\Omega^n_{y,i,j}$ are known on each grid, the constrained interpolation process can be completed according to Eqs. (20), (21) and (22).

2. After the interpolation, advection takes place, and $\Omega^{n*}_{i,j}$, $\Omega^{n*}_{x,i,j}$ and $\Omega^{n*}_{y,i,j}$ are obtained.

3. The values of $\Omega^{n+1}_{i,j}$, $\Omega^{n+1}_{x,i,j}$ and $\Omega^{n+1}_{y,i,j}$ on the mesh grid are then computed from the newly advected values in step 2 by solving the nonadvection phase of the governing equation. Then the interpolation and the advection processes are repeated.

III. Results and Discussion

In this section, we begin with the validation of code written in MATLAB language for the present method. For this purpose, we carried out prediction of fluid flow in a square cavity driven by shear force at the top boundary without the present of porous media. This type of flow configuration has been used as a benchmark problem for many numerical methods due to its simple geometry and complicated flow behaviours. It is usually very difficult to capture the flow phenomena near the singular points at the corners of the cavity.

In the simulations, two values of Reynolds number, 100 and 400 were set up defined by the height of the cavity and constant velocity of the top lid of the cavity. Benchmark solutions provided by Ghia et. al [9] were brought in for the sake of results comparison.

Fig. 2 show plots of stream function for the Reynolds numbers considered. It is apparent that the flow structure is in good agreement with the previous work of Ghia et. al [9]. For low Re ($Re = 100$), the center of vortex is located at about one-third of the cavity depth from the top. As Re increases, the primary vortex moves towards the center of cavity and increasing circular. In addition to the primary, a pair of counterrotating eddies develop at the lower corners of the cavity.

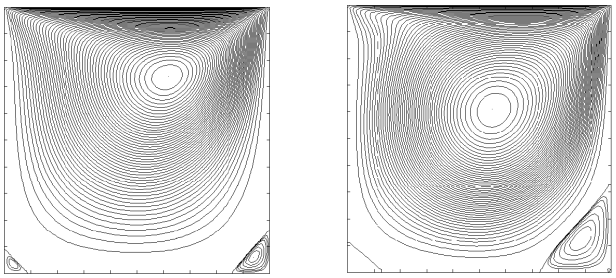

(a) (b)

Fig. 2 Plots of streamlines for (a) *Re* = 100 and (b) *Re* = 400.

The two velocity components *u* and *v* along the vertical and horizontal lines through the cavity center together with the benchmark solution are shown in Fig. 3. Good agreement between the current approach and the benchmark solutions are observed. It is noted that, the proposed approach is able to capture the critical points for the case in hand.

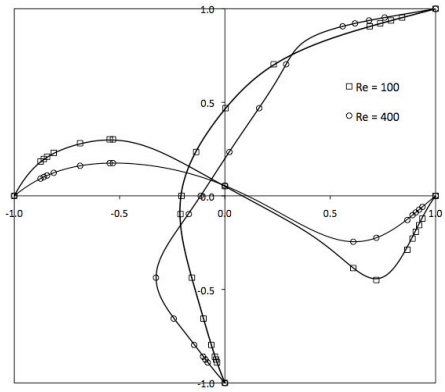

Fig. 3 Comparisons of velocity profiles between benchmark solutions (symbol) [9] and present method (solid lines)

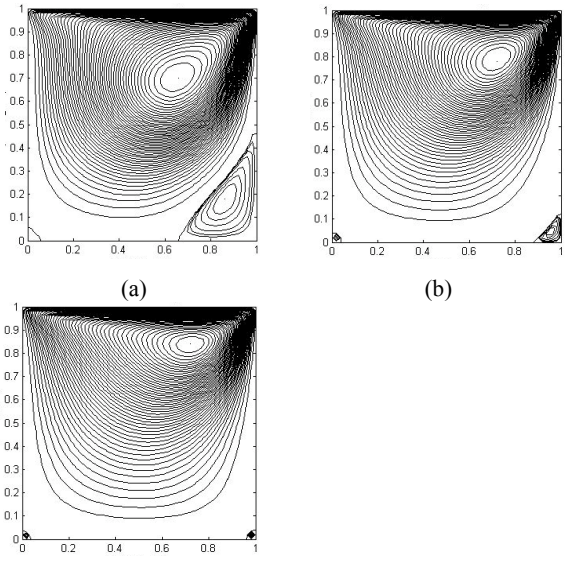

(a) (b)

(c)

Fig. 4 Plots of streamline at *Re* = 400 and (a) $\varepsilon = 0.4$ (b) $\varepsilon = 0.6$ and (c) $\varepsilon = 0.9$

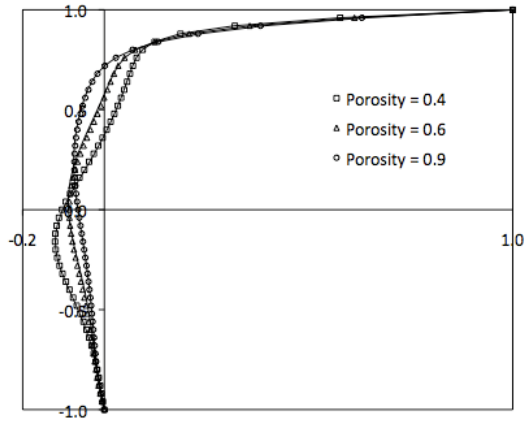

(a)

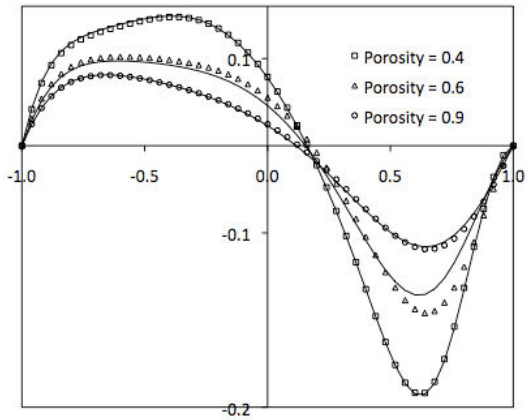

(b)

Fig. 5 Comparisons of plots of (a) horizontal and (b) vertical velocity profiles between the proposed scheme (solid line) and finite different (symbol) for *Re* = 400.

In Figs. 4 and 5, the streamline plots and velocity profiles through the cavity center are plotted for different values of porosity. For comparison, the flow is also solved by a finite-difference scheme based on a 50×50 mesh size. Clearly, the proposed solutions agree well with the finite-difference solutions for these cases. It is also seen that as value of porosity increase decreases, the boundary layer near the moving lid becomes thinner, and the vortex in the cavity becomes weaker.

IV. Conclusion

Numerical computations of fluid flow through porous media were performed using the proposed extended constrained-interpolated profile method. The results of the computations of the fluid flow in a shear driven cavity filled with porous media were compared with the finite different solutions to the flow configuration and the scheme demonstrated excellent agreement at various values of medium porosity. Future works would focus on the extension to three-dimensional scheme and prediction of fluid flow through heterogeneous porous media.

REFERENCES

[1] S. Bekri, and P. M. Adler, "Dispersion in Multiphase Flow through porous media", *International Journal Multiphase Flow*, vol. 28, no. 1, pp. 665-697, 2002.

[2] H. C. Chan, W. C. Huang, J. M. Leu, and C. J. Lai, "Macroscopic Modelling of Turbulent Flow over a Porous Medium," *International Journal Heat and Fluid Flow*, vol. 28, no. 1, pp. 1157-1166, 2007.

[3] P. Cheng, "Heat Transfer in Geothermal System," *Advanced Heat Transfer*, vol. 4, no. 1, pp. 1-105, 1978.

[4] A. Bejan, and D. A. Nield, "Convection in Porous Media," Springer, 1992

[5] K. S. Chiem, and Y. Zhao, "Numerical Study of Steady/Unsteady Flow and Heat Transfer in Porous Media using a Characteristics-Based Matrix-Free Implicit FV Method on Unstructured Grids," *International Journal of Heat and Fluid Flow*, vol. 25, no. 1, pp. 1015-1033, 2004.

[6] M. A. Seddeek, "Effects of Non-Darcian on Forced Convection Heat Transfer over a Flat Plate in a Porous Medium-with Temperature Dependent Viscosity," *International Communication on Heat and Mass Transfer*, vol. 32, no. 1, pp. 258-265, 2005.

[7] T. Seta, E. Takegoshi, and K. Okui, "Lattice Boltzmann Simulation of Natural Convection in Porous Media," *Mathematics and Computer with Simulation*, vol. 72, no. 1, pp. 195-200, 2006.

[8] P. Nithiarasu, K. N. Seetharamu and T. Sundararajan, "Natural Convective Heat Transfer in a Fluid Saturated Variable Porosity Medium," *International Journal of Heat and Mass Transfer*, vol.. 40, no. 1, pp. 3955-3967, 1997.

[9] U. Ghia, K. N. Ghia and C. Y. Shin, "High-Re Solutions for Incompressible Flow using the Navier-Stokes Equations and a Multigrid Method," *Journal of Computational Physics*, vol. 48, no. 1, pp. 387-411, 1982.

Nor Azwadi Che Sidik received the B.Eng. degree from Kumamoto University, Japan in 2001, the M.Sc. degree from University of Manchester Institute of Science and Technology, U.K., in 2003, and the PhD from Keio University, Japan, in 2007. Currently a Senior Lecturer at the Faculty of Mechanical Engineering (under the department of thermofluid), Universiti Teknologi Malaysia.

He has more than 50 publications in reputed international and national journals/conferences. His current research interests include simulation and modeling of thermal fluid flow, fluid structure interaction, numerical methods and advanced engineering mathematical theory.

Mohd Irwan Mohd Azmi received B.Eng.(Hons) degree from Universiti Sains Malaysia (USM), Penang, Malaysia in 2004, and M.Eng degree from Universiti Teknologi Malaysia (UTM), Skudai, Johore, Malaysia in 2010. Currently he is a lecturer at the Faculty of Mechanical Engineering, Universiti Teknikal Malaysia Melaka (UTeM). He has various past experiences in downstream oil and gas activity in the field of refined petroleum products distribution.

He has several publications in reputed international and national journals/conferences. His current research interests include computational fluid mechanics, convective heat transfer, liquid sloshing and renewable energy.